TUMOUR SEGMENTATION BY ACTIVE CONTOURS IN 3D CT WAVELET ENHANCED IMAGE DATA

Ioana Plajer[1,2], Tai-Khoa Nguyen-Pham[1] and Detlef Richter[1]

[1]University of Applied Sciences of Wiesbaden
Kurt-Schumacher-Ring 18, 65197 Wiesbaden, Germany, phone:+49-611-9495-1203, fax: +49-611-9495-1210,
[2]University Transilvania of Brasov,
Bulevardul Eroilor 30, 500007 Brasov, Romania, phone: +40-268 - 475590, fax: +40 – 268 - 511824,
email:iplajer@yahoo.com, richter@informatik.fh-wiesbaden.de

ABSTRACT

A method of local contrast enhancement in space frequency domain together with a segmentation method for medical 3D-CT image data by active contours is presented. The purpose of the project is to define tumor volumes for irradiation in cancer therapy. For a better performance of the contouring algorithm the image is primarily processed by a nonlinear operator in space frequency domain for local contrast enhancement.

1. INTRODUCTION

Medical image processing has become an important subject for diagnosis, surgery, irradiation planning, medical research and visualization in cancer treatment. In radiotherapy it is necessary to precisely define the target volumes for irradiation to avoid irradiating healthy tissue. For this purpose the tumors have to be segmented in all the slices of a computer tomography (CT) image data set.

The new technique of 4D-CT imaging requires the delineation of tumours in 3D data sets to reconstruct the tumour volume. The data are acquired for 12 phases of respiration. According to the size of the tumour it needs to delineate in the range of 60 to 120 2D-CT data sets.

At present no fully automatic method is efficiently segmenting medical images, therefore semiautomatic contouring methods like active contours are used. Since the first active contour model was published by Kass et. al. in [1] under the name of snake, different algorithms based on minimizing an energy function were developed. In this paper an algorithm is presented, in which the energy function was designed to optimize contour detection in CT-image data and to increase automation in target volume definition.

The main idea is to delineate the first slice of the tumour image by setting manually a starting contour for the snake. After the active contouring process, the obtained contour is transferred as a starting contour to the next slice. In each step manual corrections are allowed.

Due to the quality of the image data often some preprocessing of the image data is necessary like denoising or contrast enhancement. In this paper a method for contrast enhancement in space frequency domain is presented as an initial step before contour detection. The contrast enhancement is done by means of the wavelet transform to enhance the local contrast of different tissue regions in 3D-CT data sets.

2. MATERIALS AND METHODS

Modeling tumor volumes by active contours implies interactively defining an initial approximate contour in the region of the tumor, which will be iteratively adapted to its actual structure boundary. In certain situations the active contour is captured in the vicinity of small gradients of the tumor surface by farther located strong edges but not associated with the tumor, e.g. by bones. If the contrast at these weak edges of the tumor could be enhanced, an active contour detection will work more successfully.

2.1 Contrast enhancement using wavelet modulus maxima

The Dyadic Wavelet Transform

A good approach to local contrast enhancement is the use of wavelets, which enable localization in space frequency domain and thus the manipulation of local features. In comparison to other traditional enhancement techniques, wavelet decomposition enables higher decomposition levels to discriminate real and false edges generated by noise.

It is appropriate for edge detection application to use the dyadic wavelet transform, which results in undecimated subbands because of its translation invariance.

The 2D dyadic wavelet transform [2] can by described by convolution of the image *f(x, y)* with two wavelet functions $\psi^1(x, y)$ and $\psi^2(x, y)$ to obtain the detail sub-bands in horizontal and vertical direction and with one scaling function $\varphi(x,y)$ to obtain the approximation sub-band. For edge detection the wavelet functions should satisfy:

$$\psi^1(x,y) = \frac{\partial \theta(x,y)}{\partial x} \text{ and } \psi^2(x,y) = \frac{\partial \theta(x,y)}{\partial y} \qquad (1)$$

where $\theta(x,y)$ is a smoothing function.

Defining $\psi_s^k(x,y) = \frac{1}{s^2}\psi^k\left(\frac{x}{s}, \frac{y}{s}\right)$ for *k=1,2* then for any scale *s* the wavelet transform of $f(x,y)$ has two detail subbands:

$W_s^1 f(x,y) = f * \psi_s^1(x,y)$ and $W_s^2 f(x,y) = f * \psi_s^2(x,y)$

For the implementation of the fast wavelet transform only the dyadic sequence of scales $\left(2^j\right)_{j\in Z}$ is of interest. Taking into account (1) the detail components at each scale 2^j are given by the gradient of the convolution of the image function $f(x,y)$ with $\theta_{2^j}(x,y)$, where $0 \le j \le J$:

$$\begin{pmatrix} W_{2^j}^1 f(x,y) \\ W_{2^j}^2 f(x,y) \end{pmatrix} = 2^j \begin{pmatrix} \frac{\partial}{\partial x}\left(f * \theta_{2^j}\right)(x,y) \\ \frac{\partial}{\partial y}\left(f * \theta_{2^j}\right)(x,y) \end{pmatrix} = 2^j \vec{\nabla}\left(f * \theta_{2^j}\right)(x,y)$$

The approximation sub-band $S_{2^j} f(x,y)$ at scale 2^j is defined by convolution with the scaling function:

$$S_{2^J} f(x,y) = f * \varphi_{2^J}(x,y)$$

The dyadic wavelet transform is applied up to a certain coarse scale 2^J. At this scale a set of sub-band images $\left\{S_{2^J} f, \left(W_{2^j}^1 f\right)_{1\le j\le J}, \left(W_{2^j}^2 f\right)_{1\le j\le J}\right\}$ is available, which enable analysis and processing of details at all scales 2^j.

For the reconstruction with the inverse wavelet transform the same scaling function is used in connection with two reconstruction wavelets $\chi^1(x,y)$ respectively $\chi^2(x,y)$ [2], thus

$$f(x,y) = \sum_{j=-\infty}^{\infty}\left(W_{2^j}^1 f * \chi_{2^j}^1(x,y) + W_{2^j}^2 f * \chi_{2^j}^2(x,y)\right).$$

The fast dyadic wavelet transform is applied in practice by convolving the image with two filters *H* and *G*, corresponding to the scaling respectively to the wavelet function, both in *x* and *y* direction.

The reconstruction is done by summing the convolution of the approximation sub-band with the filter H and the convolution of the detail sub-bands with the filters K and L. The definition of these filters with respect to φ, ψ^1, ψ^2, χ^1 and χ^2 is fully described in [2]. The relations between these filter functions are given by:

$$|H(\omega)|^2 + G(\omega)K(\omega) = 1,\ L(\omega) = \frac{1+|H(\omega)|^2}{2}$$

The wavelets used in this paper are those given in [2] with the filter functions:

$$H(\omega) = e^{\frac{i\omega}{2}}\left(\cos\frac{\omega}{2}\right)^3,\ G(\omega) = 4ie^{\frac{i\omega}{2}}\sin\frac{\omega}{2}$$

Numerical values of the filter coefficients are listed in [2]. A different class of dyadic wavelets is presented in [3].

Edge points, which represent high frequency components, can be characterized by the modulus maxima of the detail sub-bands. To use this information we define for each scale 2^j the modulus $M_{2^j}(x,y)$

$$M_{2^j}(x,y) = \sqrt{\left|W_{2^j}^1 f(x,y)\right|^2 + \left|W_{2^j}^2 f(x,y)\right|^2}$$

and the angle $A_{2^j}(x,y)$

$$A_{2^j}(x,y) = \arctan\left(\frac{W_{2^j}^2 f(x,y)}{W_{2^j}^1 f(x,y)}\right)$$

of the gradient vector $\nabla\left(f * \theta_{2^j}\right)(x,y)$.

Contrast enhancement

Modification of the contrast of the image $f(x,y)$ can be achieved by applying an appropriate operator on the detail sub-bands or on the modulus at the different scales 2^j.

The interest of the contrast enhancement in this special application of tumour detection is to emphasize in space frequency domain local low contrast edges while keeping the remainder of the image regions unchanged and to avoid enhancing unwanted features.

In [4] and [5] piecewise linear operators, which are used separately on each detail sub-band, are described. In [6] and [7] nonlinear operators are presented, which favour the enhancement of low contrast regions.

The main disadvantage of most of these operators is, that contrast enhancement is not limited to a given contrast region. Another concern is to design an operator, which modifies high frequent edges and preserves low frequent structures.

The operator $\Omega_G(m)$ [8] used in this paper is based on the Gaussian function G, which allows a large enhancement within the region of interest, while the enhancement outside is small:

$$\Omega_G(m) = m + ame^{-\frac{(m-b)^2}{\sigma^2}}, \qquad (2)$$

in which the variable m represents the modulus values.

The contrast range and values are determined by parameters σ and b of the Gaussian function, while the factor of enhancement is determined by parameter a. The operator is represented graphically in figure 1.

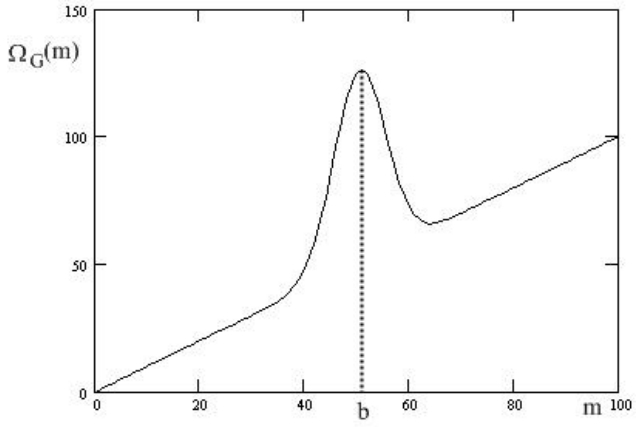

Figure 1 – Contrast enhancement operator $\Omega_G(m)$ with $a = 1.5$, $b = 50$ and $\sigma = 5$

The operator, given in eq. (2), is applied on the local maxima in the direction of the corresponding angle in the modulus image of the detail sub-bands. This results in contrast enhancement only at edges. After applying the operator, the detail sub-bands are updated from the modified modulus and the unmodified angle for each coefficient. By using the inverse wavelet transform, the enhanced image is obtained.

2.2. Active contours

For defining the tumour boundaries within an image $f(x,y)$, an active contour method is applied. This method is based on the representation of the contour as a closed parametric curve

$$v:[0,1]\to R^2,\ v(s)=(x(s),y(s))^T,\ (x(s),y(s))^T$$

are the coordinates of the control point s, characterized by an energy function. Based on this energy function the initial manually defined curve approaches the contour of the tumour by an iterative process.

In this paper the curve $v(s)$ was modelled by a closed cubic Hermitean spline, which guarantees, that the user defined control points are part of $v(s)$.

The energy function of $v(s)$

The energy function $E(v)$ of $v(s)$ is expressed by a sum of an internal, an potential and a corner energy [1,9]:

$$E(v)=E_{int}(v)+E_{pot}(v)+E_{image}(v) \qquad (3)$$

The internal energy controls the shape of the curve and is composed of an elastic and a curvature energy:

$$E_{\text{int}}(v)=E_{elast}(v)+E_{curv}(v)=$$
$$=\frac{1}{2}w_{elas}\int_0^1|v'(s)|^2\,ds+\frac{1}{2}w_{curv}\int_0^1|v''(s)|^2\,ds\,.$$

$E_{elas}(v)$ represents the tangential tension of the curve and $E_{curv}(v)$ the curvature which are weighted by the coefficients w_{elast} and w_{curv}.

The potential energy $E_{pot}(v)$ indicates to what extent the curve approaches the boundary and is based on the grey levels in the image. $E_{pot}(v)$ is expressed using the grey level gradient $P(v(s))$ by:

$$P(v(s))=\sqrt{\left|\frac{\partial f}{\partial x}(x(s),y(s))\right|^2+\left|\frac{\partial f}{\partial y}(x(s),y(s))\right|^2}$$

In discrete images the gradient can be approximated by a high-pass filter. In this application the Sobel filter was used.

The potential energy can be expressed as:

$$E_{pot}(v)=-w_{pot}\int_0^1 P(v(s))ds$$

The image energy [1] is expressed by:

$$E_{image}(v)=E_{line}(v)+E_{term}(v)=w_{line}\int_0^1 f(v(s))ds+$$
$$+w_{term}\int_0^1\frac{1}{\left(f_x^2(v(s))+f_y^2(v(s))\right)^{3/2}}\left(f_{yy}(v(s))f_x^2(v(s))-\right.$$
$$\left.-2f_{xy}(v(s))f_x(v(s))f_y(v(s))+f_{xx}(v(s))f_y^2(v(s))\right)ds,$$

in which $f_x(v(s))$, $f_y(v(s))$, $f_{xx}(v(s))$, $f_{yy}(v(s))$, $f_{xy}(v(s))$ are the corresponding partial derivatives of the image function $f(v(s))$.

When the curve $v(s)$ adheres to edges in the image, the energy is minimized. Thus the segmentation is reduced to an optimization problem.

The minimization of the energy function can be achieved in different ways. In this work minimization was performed by means of a Greedy algorithm.

In digital images the analogue functions have to be discretized. The parametric curve $v(s)$ is defined by a finite set of N control points $v_i=v(h*i)$, i = 1, ..., N-1, in which $h=1/N$ is the sampling interval. Approximating the derivative by finite differences and replacing the integral with a sum, equation (3) becomes:

$$E(v)=\sum_{i=0}^{n}\left(\frac{1}{2}w_{elas}\left|\frac{v_{i+1}-2v_i+v_{i-1}}{\Delta h^2}\right|+\right.$$
$$+\frac{1}{2}w_{curv}\left|\frac{v_{i+2}-4v_{i+1}+6v_i-4v_{i-1}+v_{i-2}}{\Delta h^4}\right|-w_{pot}P(v_i)+$$
$$\left.+w_{line}f(v_i)+E_{term}(v_i)\right)$$

with

$$E_{term}(v_i)=w_{term}\frac{1}{\left(f_x^2(v_i)+f_y^2(v_i)\right)^{3/2}}\left(f_{yy}(v_i)f_x^2(v_i)-\right.$$
$$\left.-2f_{xy}(v_i)f_x(v_i)f_y(v_i)+f_{xx}(v_i)f_y^2(v_i)\right)$$

To improve the efficiency of the contour detection a new gradient-angle energy was added to the potential energy. Considered is the angle between the grey level gradient and the actual contour, calculated by the scalar product. This energy forces the contour to move in direction of the normal vector of the curve $v(s)$ [9].

$$E_{angle}(v_i)=-w_{angle}\arccos\left(\left|\frac{(v_{i+1}-v_i)^TG(v_i)}{|v_{i+1}-v_i|\|G(v_i)|}\right|\right),$$

in which $G(v_i)=\left(f_x(v_i),f_y(v_i)\right)^T$. This energy is added to the total energy $E(v)$ and is included in the process of minimization.

Finally a balloon force [10] is applied to reduce errors, if the initial contour is not set near enough to the effective boundary or is set in a region of constant grey levels.

Minimization of the energy by a Greedy algorithm

The minimization is an iterative process working as follows: for each control point v_i of the curve the energy of the neighbouring pixels is calculated. The point v_i is then moved to the position with the smallest energy. The iteration ends if the modification of the curve in two successive steps is smaller than a defined threshold.

Improvements of the algorithm

- The elastic energy is redefined to avoid the accumulation of the curve points in local minima [11]:

  $$E_{elast}(v_i) = w_{elas}\left(d - |v_i - v_{i-1}|\right),$$

  in which d is the average distance between the neighbouring points.

- The curvature energy [11] is expressed by :

  $$E_{curv}(v_i) = w_{curv}|v_{i+1} - 2v_i + v_{i-1}|.$$

  The weight coefficient w_{curv} may be decreased locally to improve detection of tumours with strong curvature.

3. MEASUREMENTS

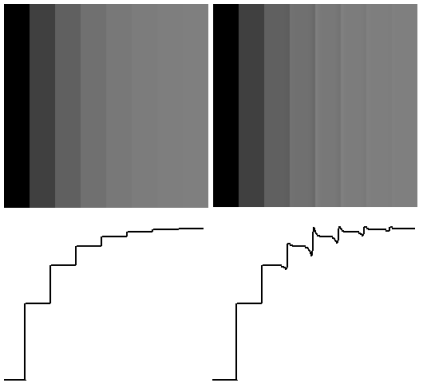

Figure 2 - Test image (left) with graph of the grey levels of an image line and processed image (right) after enhancement with an operator given in eq. (2) using parameters $\sigma = 10$ and $b = 4.5$. Parameter b is selected in dependency of the modulus maxima values. Only grey level transitions within a certain range of small grey level differences are affected.

A series of measurements was carried out to evaluate the performance of the contrast enhancement operator and the influence of its different parameters on synthetic images. It was studied how the number of scales used in the dyadic wavelet transform affects contrast enhancement in medical images.

The enhancement algorithm was first tested on synthetic computer generated images. It was observed, that modifying the details at the first decomposition level will significantly increase noise, while using only the following decomposition levels gives a better result. Using more than 3 decomposition levels in the wavelet transform increases computational effort, but does not affect the results significantly, so in the algorithm the scales used were reduced to the first 3 subbands, from which only the second and the third were modified.

In figure 2 the local enhancement at a certain contrast range of the operator, given in eq. (2), is illustrated. By applying the operator the grey level contrast is enhanced only in a small range of grey level differences. Smaller or larger grey level differences remain unaffected. By varying parameter σ the width of grey level differences is changed. The parameter b controls the position of the maximum enhancement. Its value is selected in dependency with the features that have to be enhanced.

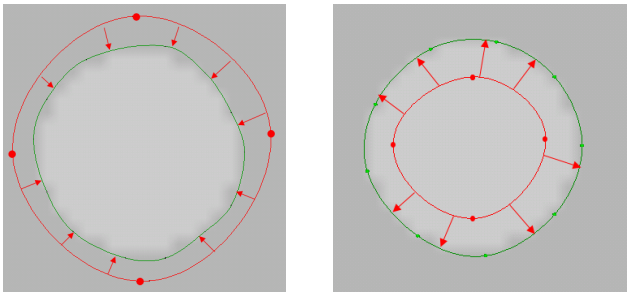

Figure 3 – Active contour detection on test image with starting contour outside the structure (left) and starting contour inside the structure (right).

The active contour algorithm was tested at first with test images of a sphere, with different starting contours, e.g. a starting contour outside and inside of the structure to be detected. In figure 3 the results of such a test are given.

Some more tests were done to verify the improvement obtained from adding the gradient angle energy and the balloon force [9].

4. RESULTS AND DISCUSSIONS

The segmentation in the proposed version of the active contouring was tested on several lung tumours with different shapes and on other anatomical structures like the prostate. Figure 4a) shows a tumour completely inside the soft lung tissue. The tumour is separated from the surrounding tissue by good contrast in most parts of the contour. In figure 4b) a tumour, adherent the thorax wall, is shown. Contrast differences between tumour and lung tissue respectively the thorax wall vary very much and demand high sophisticated algorithms to detect the correct tumour boundary. Figure 4c) shows a ramified lung tumour. Figure 4d) shows a prostate with only low contrast to the surrounding tissue and high contrast structures in its vicinity.

The results were compared with manually delineations done by an expert radiologist. Using a similarity index:

$$SI = \frac{V_A \cap V_B}{V_A \cup V_B},$$

in which V_A and V_B are the automatically and the manually delineated volumes respectively, we found indices in the range of 75% to 85% [9].

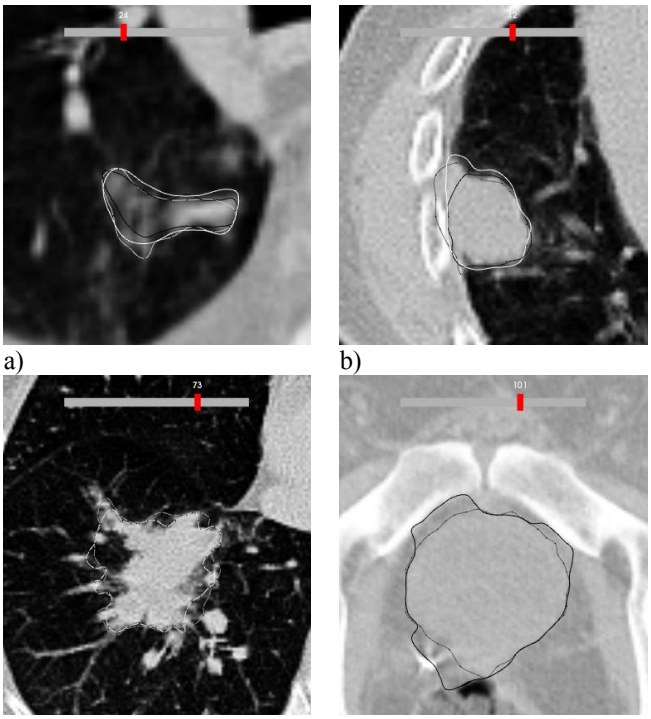

Figure 4 – a)-c) Segmented lung tumours d) Segmented prostate. The contours detected before and after contrast enhancement are dark grey respectively light grey. The white contours in a) and b) are the manually delineated contours by an expert radiologist.

5. CONCLUSIONS

In this work we presented a combination of active contours with wavelet decomposition and reconstruction to enhance image contrast within a certain range of grey level differences. The aim is to decrease time consuming interactions by the radiologists during a delineation process. We focussed on 4D-CT images of lung tumours in which the resulting contours of the precedent image slice is transferred as starting contour for the subsequent slice.

To judge the results, it must be ensured, that the contouring algorithm reproduces the same or nearly the same tumour boundaries when it is repeatedly applied. In cases of low contrast images and when the starting contour was defined by different data point positions or when or the tumour structure was too irregular, this was not always achieved.

In figure 4 a) and b) in the wavelet enhanced images the automatically produced grey contours fit better to the white contours, which were defined manually by an expert radiologist, than the dark grey contours, which were produced without enhancement.

In figure 4 c) it may be seen, that for ramified structures neither the active contours without enhancement nor the contours with enhancement fit the real boundary of the tumour.

In figure 4 d) the grey contour obtained after wavelet enhancement is much closer to the prostate boundary then the dark grey contour produced before enhancement.

It is necessary to define standardized parameters for the active contouring and the wavelet enhancement as well, depending on different models of tumour situations.

In the case of contouring the lung tumours we used a model based reduction of parameters down to two parameters. These two parameters could be applied to all of the 60 to 120 2D-CT images of the same 4D-CT data set.

In the case of strongly ramified tumours, the number of control points for active contouring must be adapted accordingly.

REFERENCES

[1] M. Kass, A. Witkin and D. Terzopoulos, "Snakes: Active Contour Models", *International Journal of Computer Vision*, pp. 321-331, 1988.

[2] S.Mallat, S Zhong, "Characterization of Signals from Multiscale Edges," *IEEE Transactions on Pattern Analysis and Machine Intelligence*, vol. 14, No. 7, pp. 710–732, July 1992.

[3] B. Chiu, *A New Segmentation Algorithm for Prostate Boundary Detection in 2D Ultrasound Images*. Master-Thesis, Waterloo, Ontario Canada, 2003.

[4] A. Laine, J. Fan and W. Jang, "Wavelets for Contrast Enhancement of Digital Mammography," *IEEE Engineering in Medicine and Biology*, pp.536–550, September/October 1995.

[5] A. Mencattini, M. Salmeri, R. Lojacono and F. Caselli, "Mammographic Image Enhancement and Denoising for Microcalcification Detection using Dyadic Wavelet Processing," in *Proc. IMTC-Instrumentation and Measurement Technology Conference*, Sorrento, Italy, April 24-27, 2006, pp. 49-53.

[6] P. Sakellaropoulos, L. Costaridou and G. Panayiotakis, "A Wavelet-Based Spatially Adaptive Method for Mammographic Contrast Enhancement," *Physics in Medicine and Biology*, vol. 48, pp. 787-803, 2003.

[7] X. Zong, A.Laine, "De-noising and Contrast Enhancement via Wavelet Shrinkage and Nonlinear Adaptive Gain" in *Wavelet Applications III, Proc. of SPIE*, Orlando, Florida, USA, April 8-12, 1996, vol. 2762, pp. 566-574.

[8] I. C. Plajer, D. Richter " Contrast Enhancement in Space Frequency Domain for Active Contouring of CT Data Sets Using Wavelet Transform", *Proc. of DSC 2009,* Thessaloniki, Greece, July 2009

[9] T. K. Nguyen-Pham, "Semiautomatische Konturierung von Lungentumoren mit Hilfe aktiver Konturen in 3D-CT Aufnahmen für die Hochpräzisionsbestrahlung", *Diploma-Thesis,* University of Applied Sciences of Wiesbaden, Germany 2009

[10] L.D. Cohen, "On Active Contour Models and Balloons", *Computer Vision, Graphics and Image Processing: Image Understanding*, vol. 53(2), pp. 211-218, March 1991

[11] P. Tiilikainen, "A Comparative Study of Active Contour Snakes", Copenhagen University, Danmark, 2007